Chemistry Research Journal, 2023, 8(4):1-12
Available online www.chemrj.org

Research Article

ISSN: 2455-8990
CODEN(USA): CRJHA5

Molecular and crystal structure of Methylene Blue Tetrachloridocobaltate (ii) and intermolecular π-π stacking interactions Energy

Vahobjon Kh. Sabirov*, Mukarram X. Kadirova

Chemistry department, Institute of Pharmaceutical Education and Research, Tashkent, Uzbekistan
*Corresponding author. E-mail: v_sabirov@mail.ru & vahobjonsabirov15@gmail.com

Abstract
Tetrachloridocobaltate(II) complex $[MB]^{+2}[CoCl_4]^{2-}$ (where [MB]+–methylthioninium cation; methylene blue cation) was synthesized as a result of the mechanochemical reaction of $CoCl_2.6H_2O$ hexahydrate with $[MB]Cl{\cdot}5H_2O$. The crystal structure of the title compound was studied by single-crystal X-ray diffraction study, FTIR spectroscopy, the Hischfeld surfaces analysis. The asymmetric unit of the studied compound consists of a $[CoCl_4]^{2-}$ anion and two $[MB]^+$ cations. One of Cl^- anions is disordered over two positions. Coordination polyhedron of the central atom is a highly flattened tetrahedron. The planar $[MB]^+$ cations are stacked in an antiparallel mode with sulfur atoms disposed alternatively on opposite sides, and exhibiting π-π stacking at the average interplanar distances of 3.482 Å. The Hirshfeld surface analyzes shown that the highest contribution of total HS is attributed to H···H interactions with 46.7 and 46.8 % for each MB^+ cation. Intermolecular interaction energy E were computed for two neighboring π-π associated MB+ cations using a dispersion-corrected CE-B3LYP/-31G(d, p) level of theory available in CrystalExplorer17.5 program.

Keywords: Cobalt chloride, methylene blue, mechanochemical synthesis, Hirshfeld surface, π-π interaction

1. Introduction

Methylene blue ($[MB]^+$ - methylthioninium cation; 3,7-bis(dimethylamino)-phenothiazin-5-ium), a blue-colored a phenothiazine derivative was first developed for the dyeing of cotton fibers [1].

However, in addition to coloring properties, this compound has many biological and therapeutic properties, which are described in detail in reviews [2, 3].

The $[MB]^+$ cationic ligand has N and S atoms as possible electronic donor centers. However, the coordination of the MB+ ligand to the central atom is observed only in a Cu(I) complex, and the MB^+ cation coordinates the copper atom through the N atom of the central ring [4].

The salt type complexes of Hg(II) [5], Ag(I) and Au(I) chlorides [4] with the MB^+ counterion were also prepared and studied by single crystal X-ray diffraction (XRD) way.

We have recently obtained three complexes of copper (I, II) with MB and studied them by XRD [6]. This paper presents results of an XRD study of the complex $[MB]^{+2}$ $[CoCl_4]^{2-}$ (I).

2. Experimental Section

2.1. Materials and Methods

All reagents were readily available from commercial sources and were used as received without further purification. Analysis of C, H and O were performed on a German Elementar Vario EL instrument. The Fourier Transform-Infrared (FT-IR) spectra were recorded on Shimadzu IR- MIRacle-10 spectrophotometer in the range of 400–4000 cm−1.

2.2. Synthesis and crystallization

The complex I has been obtained as a result of the mechanochemical reaction of $CoCl_2.6H_2O$ with [MB]Cl × $5H_2O$ that eliminate the adverse effect of the solvent on the course of the reaction. Reagents $CoCl_2.6H_2O$ (23.80 mg, 0.1 mmol) and [MB]Cl×$5H_2O$ (82 mg, 0.2 mmol) in a 1:2 stoichiometric ratio were ground in an agate mortar until a gold-like thin mass was formed. 5.0 ml of DMF was gradually added drop wise to the reaction mixture and the process was continued until a homogeneous dark blue solution was formed. The resulting solution was transferred into an evaporation dish and allowed to evaporate slowly at room temperature for one week and after that, the dark blue color crystals were isolated. Yield: 75%. Elemental analysis for $C_{32}H_{38}CoCl_4N_6S_2$ (769.52): calcd. C 66.40; H 4.9; N 10.9 %; found: C 65.65; H 4.69; N 10.6 %.

The Fourier Transform-Infrared (FT-IR) spectra were recorded on Shimadzu IR MIRacle-10 spectrophotometer in the range of 400–1800 cm^{-1}.

FTIR (ATR), cm^{-1}: 1645(ν(=N=(CH3)2), 1587 (νhet(C-N)), 1487 (ν (C=S+)), 1419 (δ(CH), δ(CH), 1244 (δ(CH), γ(C-H)), 1164 (δhet(C-C)), 1134 (δhet(C-N)), 1056, 949.5, 823.4, 689.15, 791.47, 666.9, 617.5, 534.1, 416 cm^{-1}.

2.3. The single crystal X-ray diffraction experiment and the solution of crystal structure (I)

The X-ray diffraction experiment was carried out on an 'XtaLAB Synergy, HyPix3000' diffractometer (CuKα-radiation, λ = 1.54184 Å, ω scan mode, mirror monochromator, at T = 299 K) [7].

The crystal structures were solved with OLEX2 [8] using the program SHELXTL [9], and refined by full-matrix least-squares method on F2 using the SHELXL refinement package [10].

All non-hydrogen atoms were refined anisotropically. The H atoms of the CH_3-groups were included in calculated positions and refined as riding: C–H = 0.95–0.98 Å with Uiso(H) = 1.5Ueq(C-methyl) and 1.2Ueq(C) for other H atoms. The positions of disordered Cl atoms defined from the difference Fourier map of the electron density and refined anisotropically. All details of the diffraction experiment and crystal structure solution are presented in Table 1.

Table 1: Crystal data and structure refinement details for I.

Empirical formula	$C_{32}H_{36}N_6Cl_4CoS_2$
Formula weight	769.52
Temperature/K	293(2)
Crystal system	monoclinic
Space group	$P2_1/n$
a, Å	15.1315(8)
b, Å	14.9413(6)
c, Å	16.5119(9)
β, deg.	115.265(5)
Volume, $Å^3$	3376.0(3)
Z	4
$\rho_{calc,}$ $g{\cdot}cm^{-3}$	1.5
μ, mm^{-1}	8.322
F(000), *e*	1588.0
Crystal size (/mm^3)	0.3 × 0.2 × 0.2
Radiation	Cu*K*α (λ = 1.54184)

2θ range for data collection, deg.	6.642 to 143.112
Index ranges	$-18 \le h \le 13, -17 \le k \le 18, -20 \le l \le 20$
Reflections collected	37080
Independent reflections	6565 [R_{int} = 0.2301, R_{sigma} = 0.1685]
Data; restraints; parameters	6565; 0; 416
Goodness-of-fit on F^2	0.952
Final R indexes [$I>=2\sigma(I)$]	R_1 = 0.0820, wR_2 = 0.1609
Final R indexes [all data]	R_1 = 0.2355, wR_2 = 0.2372
Largest diff. peak; hole -e·Å^{-3}	0.54; -0.33

2.4 Hirshfeld surface (HS) and intermolecular interaction energy calculations

3D-HS and related 2D fingerprint plots were generated for the title compound based on the crystallographic information file (CIF) using CRYSTALEXLORER17.5 [11-13]. The molecular 3D-HS for [MB]+ cations are mapped over the dnorm (−0.2074 to −1.5134 a.u.), de (−1.0154 to 2.6214 Å), shape index (−1 to 1 a.u.), curvedness (−4 to 0.4 Å) and fragment pathch (0 to 4Å).

The interaction energy between π-π stacked [MB]+ cations for the title compound had been calculated using the CRYSTALEXPLORER17.5 software in the 3LYP/6-31G(d,p) and HF/3-21G levels of theory [13].

3. Results and Discussion

3.1. Molecular structure description

Cobalt(II) and copper(II) cations have similar effective ionic radii so they form with MBCl isostructural, pseudotetrahedral complexes. Complex (I) is isostructural with the complex $[MB]^{+2}$ $[CuCl_4]^{2-}$ (II) which was discussed in [11]. The cell parameters of both crystals are similar: a=15.1404(7), b= 14.9566(4), c= 16.5237(8) Å, β= 115. 279(6)°, V= 3383.5(3) Å3 for I; a=15.1327(5), b=14.9456(3), c=16.5175(5), β=115.236(4), V= 3379.18(19) Å3 for II.

As shown in Fig.1, the crystal structure of I composed of $[CoCl_4]^{2-}$ anion and two symmetry-independent $[MB]^+$ cations. The Co coordination sphere is not a perfect tetrahedron. Here, the coordination sphere is distorted with respect to both bond lengths and angles: the Co–Cl distances vary in the range of 2.242(4)–2.265(3) Å and the Cl–Co–Cl bond angles vary in the range of 96.26(12) – to 139.65(14)°. In the crystals I and II, the M–Cl bond lengths are very similar. Selected bond lengths and bond angles in I are listed in Table 2.

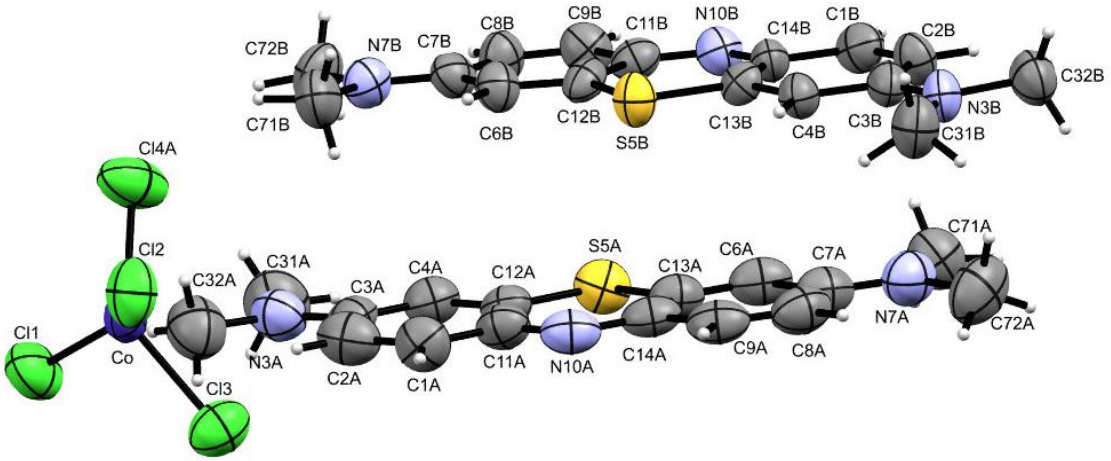

Figure 1: Molecular structure and atom numbering scheme for the compound I. Displacement ellipsoids are drawn at the 50% probability level. The disordered Cl^- ion with a low population is omitted. The atoms of the independent $[MB]^+$ cations are designated by symbols A and B for clarity.

One of the Cl- ions coordinated to an atom Co, is disordered over two positions Cl_4A and Cl_4B with occupation factors 0.91(1) and 0.09(1).

The distortion of the $[CoCl_4]^{2-}$ coordination polyhedron from a regular tetrahedron can be attributed to the asymmetric arrangement of p donors of hydrogen bonds in crystal I.

The $[MB]^+$ cations, as commonly seen in other related compounds, is planar and neighboring that are stacked in an antiparallel fashion with the sulfur atom disposed alternatively on opposite sides, and exhibiting π–π stacking at an average distance of 3.482 and 3.478 Å for different pairs. The centroid distances between adjacent $MB(A)^+$ and $MB(B)^+$ cations is 4.015 Å, between two neighboring $MB(A)^+$ cations is 4.077 Å, and between two adjacent $MB(B)^+$ cations is 4.476 Å (Fig. 2).

In the π-π stack, the dihedral angle between average planes (except of H atoms) of the neighboring $[MB(A)]^+$ and $[MB(B)]^+$ cations is 2.1º.

Table 2: Selected bond lengths (d) and bond angles (ω) in the structure (I).

Bond	***d*, Å**		**Bond**	***d*, Å**	
Co–Cl	2.262(3); 2.266(3); 2.255(3); 2.247(3); 2.18(4)				
	$[MB(A)]^+$	$[MB(B)]^+$		$[MB(A)]^+$	$[MB(B)]^+$
S5–C12	1.725(9)	1.732(8)	S5–C13	1.720(9)	1.726(8)
N3–C3	1.347(12)	1.343(10)	C7–N7	1.356(12)	1.354(10)
N10–C11	1.325(11)	1.325(11)	N10–C14	1.352(11)	1.347(10)
Angle			ω,˚		
Cl–Co–Cl	85.2(11) – 165.1(14);				
	$[MB(A)]^+$			$[MB(A)]^+$	
C12–S5–C13	103.8(5)			104.0(4)	
C10–N11–C14	123.8(8)			124.0(7)	

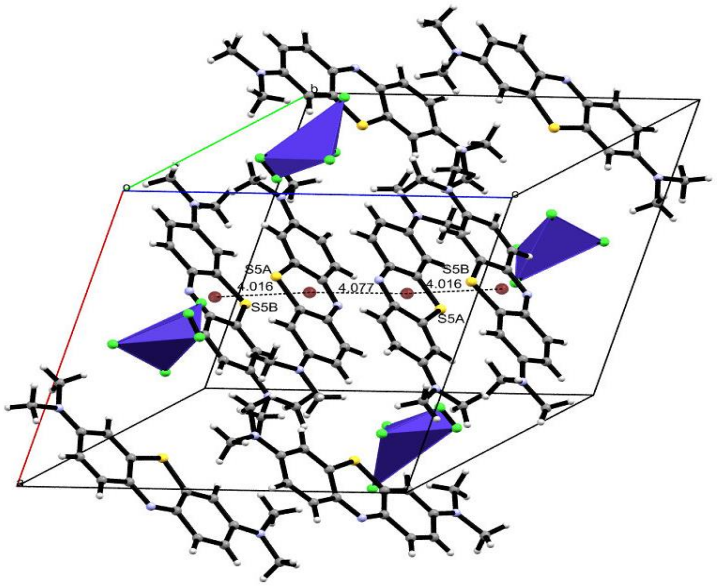

Figure 2: Crystal packing of the complex I and centroid-centroid distances

The C11–N10–C14 (123.8(8) and 124.0(7)º) and C12–S5–C13 (103.8(5) and 104.0(4)º) bond angles are close in both cations. These parameters negligible distinguish from corresponding parameters found in the crystalline phenothiazine, where the C–N–C bond angle is 124.4(5)° and the C¬–S–C bond angle is 100.9(3)° [14].

The angles between the principal axes of the adjacent $[MB(A)]^+$ and $[MB(B)]^+$ cations is about 16º. Obviously, symmetrically related MB^+ cations are arranged strictly antiparallel.

The $[CoCl_4]^{2-}$ anion is located between π-π stacks of the MB^+ cations and form short contacts with neighboring $[MB]^+$ cations via the C-H…Cl type hydrogen bonds. Geometrical parameters of the short contacts are presented in Table 3.

Table 3: The geometry of short contacts in the crystal structure of I.

D-H…A	D–H, Å	H…A, Å	∠D–H…A,°	D…A, Å	Symmetry
C72B-H…S5B	0.96	2.85	143	3.668(5)	[-*x*+3/2, *y*+1/2, -*z*+1/2]
C72B-H…Cl1	0.96	2.85	169	3.797(4)	[*x*-1/2, -*y*+3/2, *z*-1/2]
C2B-H…Cl2	0.93	2.60	166	3.510(4)	[*x*-1, *y*, *z*-1]
C31A-H…Cl3	0.96	2.89	169	3.834(4)	[-*x*+3/2, *y*+1/2, -*z*+3/2]
C31A-H…Cl1	0.96	2.85	141	3.649(4)	[*x*-1/2, -*y*+3/2, *z*-1/2]
C32B-H…Cl2	0.96	2.73	161	3.658(4)	[*x*-1, *y*, *z*-1]
C8B-H…Cl4	0.93	2.81	143	3.595(4)	[*x*-1/2, -*y*+3/2, *z*-1/2]
C8A-H…Cl3	0.93	2.84	134	3.551(4)	[*x*-1/2, -*y*+1/2, *z*-1/2]
C2A-H…Cl3	0.93	2.80	144	3.591(5)	
C4B-H…Cl2	0.93	2.88	162	3.776(5)	[*x*-1/2, -*y*+1/2, *z*-1/2]
C32A-H…S5A	0.96	3.01	167	3.948(5)	[*x*+1/2, -*y*+3/2, *z*+1/2]
C31B-H…Cl4	0.96	2.85	143	3.652(4)	[-*x*+3/2, *y*-1/2, -*z*+1/2]
C31B-H…Cl2	0.96	2.80	151	3.669(4)	[*x*-1/2, -*y*+1/2, *z*-1/2]

3.2. Hirshfeld surface (HS) analysis

The dnorm surface was obtained with a red-white-blue color scheme for dimer of the $[MB(A)]^+$ and $[MB(B)]^+$ cations in the asymmetric unit, where red indicates the shorter intermolecular contacts, white shows the contacts around the van der Waals (vdW) radii separation and blue represents the longer intermolecular contacts. Based on the local curvature of the molecular surface extra colored properties, shape index and curvedness can also be quantified.

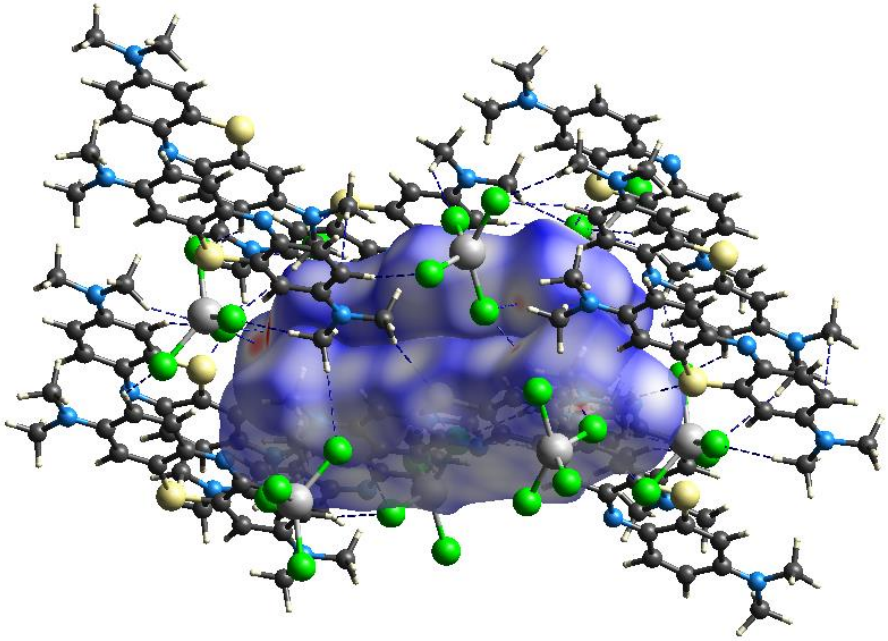

Figure 3: A view of the 3D Hirshfeld surface of the compound I mapped over dnorm.

As shown in Fig. 3, the majority of dnorm surface is colored white (representing interatomic contacts with distances around the vdW separation, i.e. the H···H and C–H···S contacts, and remaining features are light-blue corresponding to longer contact distances. A few light-red spots on that surface indicate the contact points with atoms participating in intermolecular weak C–H···Cl contacts.

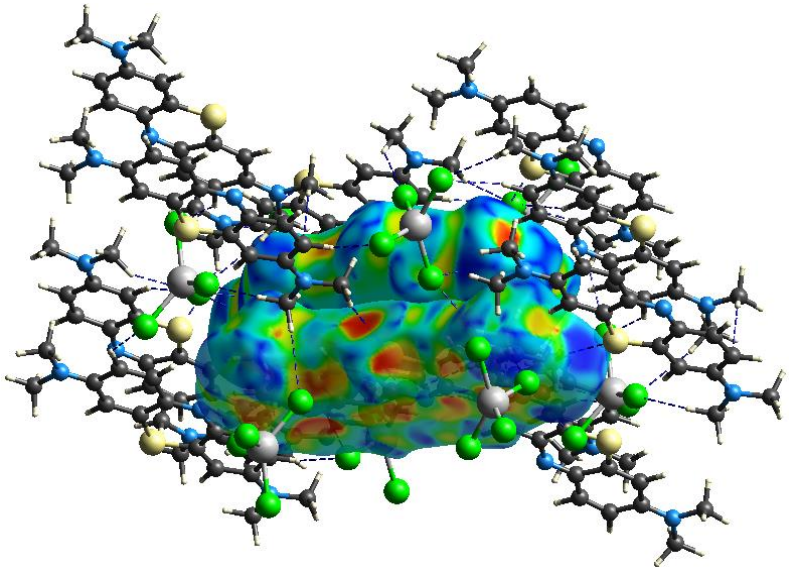

Figure 4: Shape index for a pair of the $[MB]^+$ cations

On the shape-index surface, convex blue regions represent hydrogen-donor groups and concave red regions represent hydrogen-acceptor groups. This surface is a tool to visualize π–π stacking by the presence of adjacent red and blue triangles; if there are no adjacent red and/or blue triangles, and then there are no π–π interactions. Fig. 4 clearly suggests that there are π–π interactions in the crystal I (blue ellipse). The blue triangles represent convex regions resulting from the presence of ring carbon atoms of the molecule inside the surface, while the red triangles represent concave regions caused by carbon atoms of the $[MB]^+$ cation above.

This interaction is shown as a relatively large and flat green region on the corresponding curvedness surface at the same side of the molecule, and confirms the presence of π···π interactions (Fig. 5).

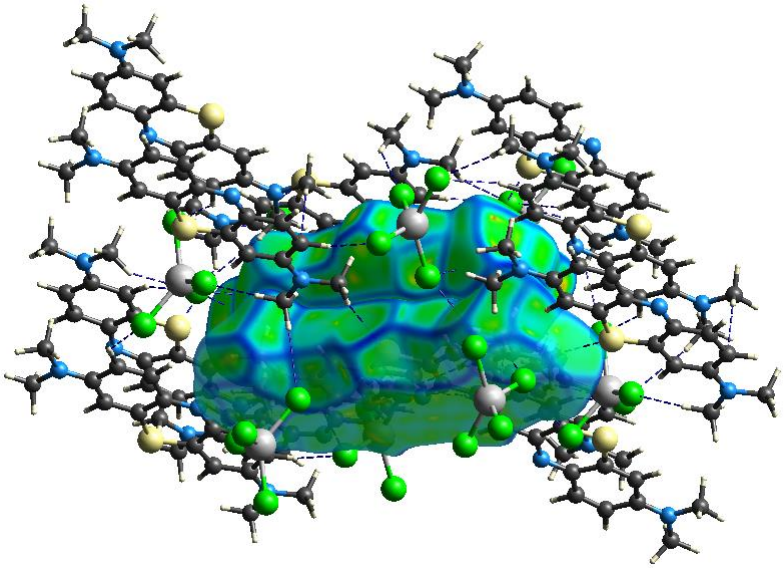

Figure 5: The 3D-HS for a pair of the [MB]+ cations plotted with curvedness.

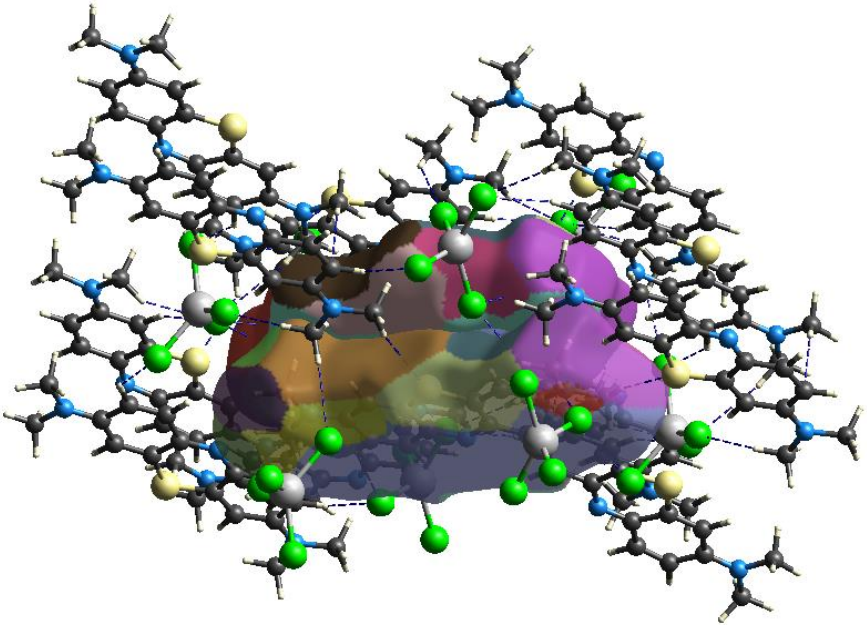

Figure 6: Fragment patch of a pair of the [MB]+ cations in the crystal of I.

The nearest adjacent coordination environment of the molecules is identified from the color patches on the Hirshfeld surface based on their closeness to adjacent molecules. Therefore, the fragment patches show the appropriate approach for the identification of the nearest neighboring coordination environment of the [MB]+ cation (Fig. 6).

The HS of a [CoCl4]2- anion was built to visualize short contacts formed by this anion with adjacent [MB]+ cations. On the dnorm surface, the bright red spots clearly show an intermolecular C-H…Cl contacts between methyl groups of [MB]+ cations and [CoCl4]2- anion (Fig. 7). Weak interactions with the atom···atom separations longer than a sum of van der Waals radii of the contacting atoms are presented by pale red spots.

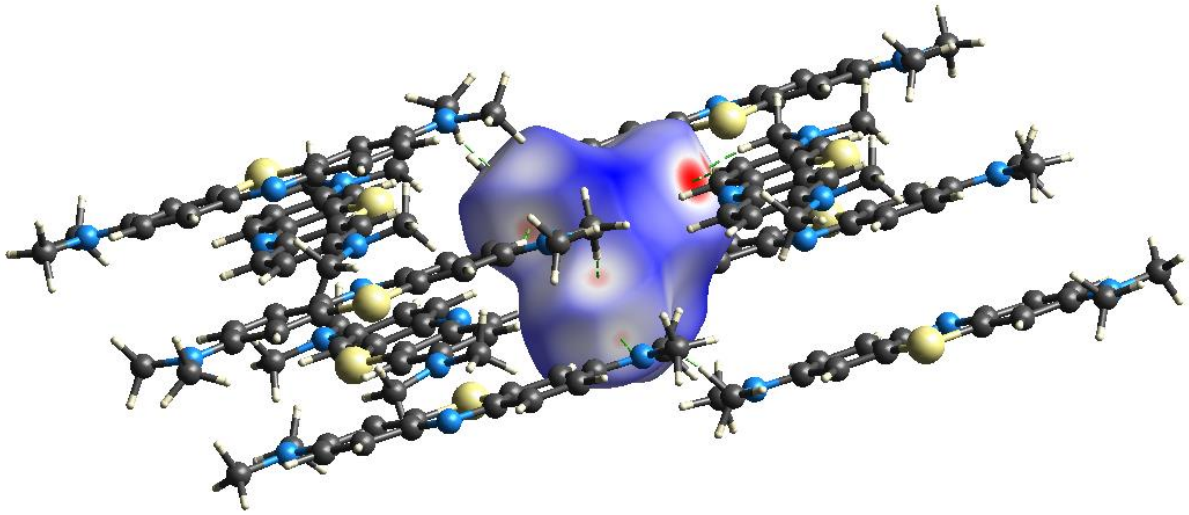

Figure 7: The HS surface of a [CoCl4]2- anion mapped over dnorm.

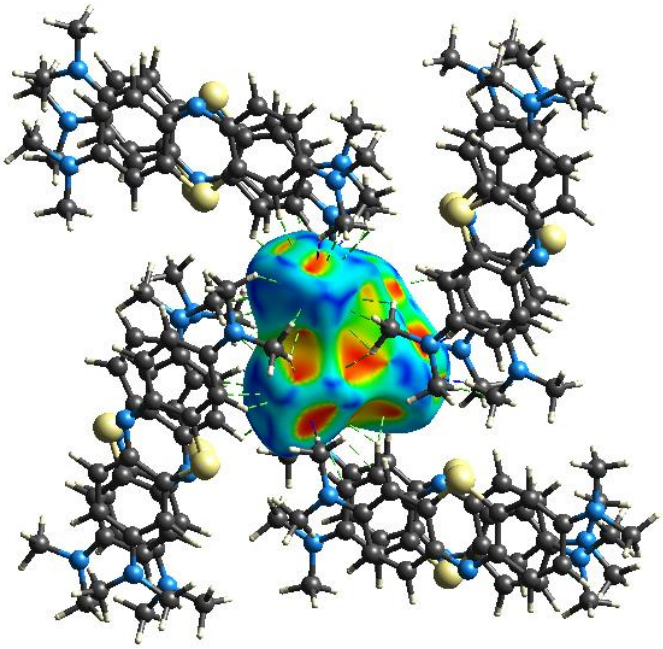

Figure 8: The 3D-HS of a [CoCl4]2- anion mapped with shape-index.

The C-H…Cl interactions between the methyl group and a $[CoCl_4]^{2-}$ anion is evident in the HS mapped over shape-index of the bright red area (Fig. 8).

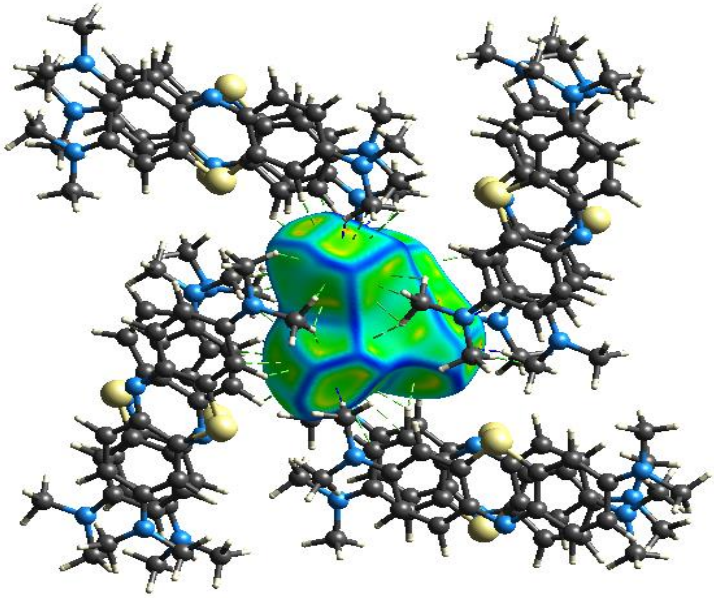

Figure 9: The 3D-HS of a $[CoCl_4]^{2-}$ anion plotted with curvedness

In the curvedness maps, relatively large green planes separated by blue edges are shown in the regions where methyl groups of the dimethylamino groups of the $[MB]^+$ cation and $[CoCl_4]^{2-}$ anion are located. As seen in Fig. 9, the areas of sharp curvature have a high curvedness and divide the surface into patches associated with separate contacts between neighboring molecules.

The nearest neighboring coordination environment of the $[CoCl_4]^{2-}$ anion is defined from the color patches on the Hirshfeld surface mapped with the fragment patch based on their closeness to adjacent molecules (Fig. 10).

Therefore, the fragment patches show the appropriate approach for the identification of the nearest neighboring coordination environment of the $[CoCl_4]^{2+}$ anion.

The quantitative analysis of the percentage of the Hirshfeld surface-associated 2-D finger prints with a particular atom-pair interaction provides a summary of the frequency of each combination of de and di across the surface of a molecule. These findings specify the various types of interaction present and its relative area on the surface.

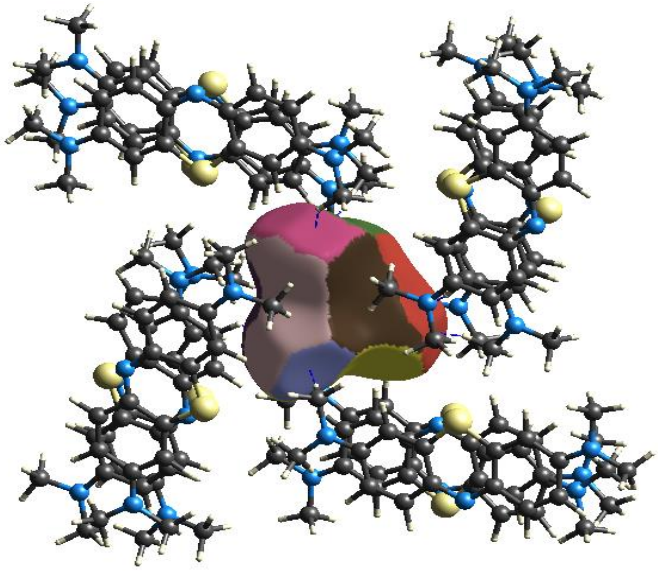

Figure 10: The HS of a $[CoCl_4]^{2-}$ mapped patch surface

The contributions of various intermolecular interactions to the total crystal packing are presented in Table 5. As can be seen from this table, the same types of interactions make almost equal contributions to total intermolecular interactions for both MB cations, and in both cases, the main contributions to total intermolecular interaction are made by the H...H contacts (46.7 and 46.8% for $[MB(A)]^+$ and $[MB(B)]^+$, respectively) (Table 5).

The C---C contact between neighboring cations make a low contrbution to the Hirshfeld surface which is 7.9 (MB(A)) and 8.1 (MB(B)) %. Because of the repulsion interaction of the dimethylamino groups, the aromatic cycles of the $[MB]^+$ cations overlap partly due to the repulsion of the methylamine groups and the principle axis of the neighboring $[MB]^+$ cations are rotated mutually.

As seen from Table 5 and Fig. 11, the total Hirschfeld surface maps are similar both $[MB]^+$. The persantage contributions of the C---C intercationic contacts to total intermolecular interactions are almost equal: 7.9 and 8.1% for $[MB(A)]^+$ and $[MB(B)]^+$ cations.

The H---H contacts make the major persentage contributions into intermolecular contacts: 46.7 and 46.8 %, for $[MB(A)]^+$ and $MB(B)^+$ cations respectively (Table 5, Figs. 11 and 12)

Table 5: Percentage contribution to the total Hirshfeld surface area of the [MB]+ cations.

Interaction	[MB(A)]	[MB(B)]	Interaction	[MB(A)]	[MB(B)]
H…H	46.7	46.8	C…C	7.9	8.1
H…Cl	13.9	14.7	C…N/N…C	3.6	3.0
H…C/C..H	12.5	12.7	C…S/S…C	2.9	2.5
H…S/S…H	6.1	6.0	N…S/S…N	0.1	0.2
H..N/N…H	4.7	5.3	S…Cl	0.3	0
C…Cl	0.2	0	N…Cl	0.2	0.1

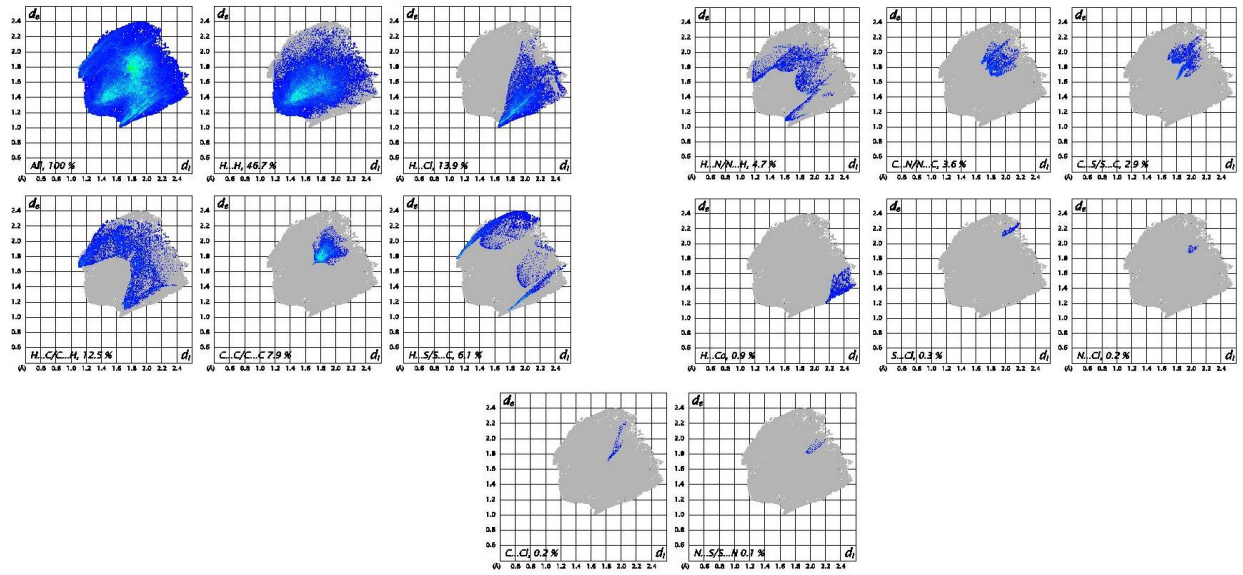

Figure 11: 2-D fingerprint plots showing percentage contribution to the total Hirshfeld surface area of the [MB(A)]$^+$ cation.

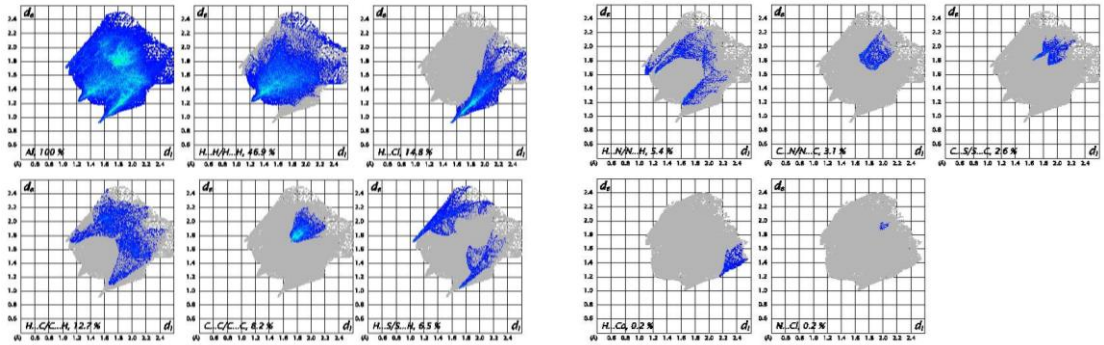

Figure 12: 2-D fingerprint plots showing percentage contribution to the total Hirshfeld surface area of the [MB(B)]$^+$ cation.

3.3. Intermolecular interaction energy calculations

The dimerization and higher order aggregates of methylene have been very widely studied by UV-Visible spectroscopy in aqueous, pure and mixed organic solvents for many years [15, 16]. These phenomena are of interest for a wide range of practical applications, such as chemical indicators, markers and spectral sensitization systems, biocompatible agents for photodynamic therapy.

The π-π stacking of [MB]$^+$ cations occurs in all crystals of MB compounds studied by X-ray diffraction analysis [4, 5, 6, 17, 18], however, the interaction energy between π-π stacked pairs of [MB]$^+$ cations has not yet been calculated.

The calculation of the interaction energy between two π-π stacked [MB]$^+$ cations makes it possible to understand the nature of the forces acting between the [MB]$^+$ cations. The total intermolecular energy Etot, which is correlative to the [MB]$^+$ cation, is the sum of four main energy components comprising electrostatic (Eele), polarization (Epol), dispersion (Edis) and exchange-repulsion (Erep).

In the crystal structure I, the π-π interaction energy between adjacent [MB]$^+$ cations had been calculated using the CRYSTALEXPLORER17.5 software in the B3LY/-31G(d,p) and HF/3-21G levels of theory.

The obtained energy values are presented in Table 5. As can be seen from this table, the energies obtained in the two approaches have different values. The B3LY/-31G(d,p) theoretical level is more suitable for estimating the π-π stacking interaction energy between two cations in crystal I.

The calculations shown that the π-π stacking interaction energy Etot between two neighboring $[MB(A)]^+$ cations is -86.7 kJ/mol, between two neighboring $[MB(B)]^+$ cations is -77.8 kJ/mol, and between the $[MB(A)]^+$ and $[MB(B)]^+$ cations is -53.5 kJ/mol. Among all interaction energies, the dispersion energy is dominant in comparison with other types of the intermolecular interactions. It is greater than the sum of all repulsive energies in π-π stacking interactions of the $[MB]^+$ cations in all cases considered.

Table 6: Interaction energy between two the [MB]+ cations in the crystal I.

N	Symop	R	Electron Density	E_ele	E_pol	E_dis	E_rep	E_tot
1	-	3.85	B3LYP/6-31G(d,p)	0.95	-18.65	-87.1	51.30	-53.5
1	-	3.85	HF/3-21G	0.92	-16.4	-90.1	67.31	-38.3
1	-	3.85	B3LYP/6-31G(d,p)	13.2	-25.2	-100.0	73.2	-46.5
1	-x, -y, -z	4.68	B3LYP/6-31G(d,p)	-30.5	-21.9	-88.9	63.3	-86.7

4. Conclusions

During the solution-assistance mechanochemical synthesis of cobalt chloride with methylene blue has been obtained a salt-type complex $[MB]^{+2}[CoCl_4]^{2-}$. Chemical composition and structure of the complex were determined by the single crystal X-ray diffraction crystallograhy. The $[MB]^+$ cations are planar and stacked in an antiparallel fashion with the sulfur atom disposed alternatively on opposite sides, and exhibiting π–π stacking with average intercationic separations 3.482 and 3.47 Å. The 3D-HS and 2D fingerprint analysis reveal that percentage contribution of the C-C closest contacts of the $[MB]^+$ cations is about about 8 %. Intermolecular interaction energy calculated for two MB(A) cations is -87.7 kJ/mol, and stacking interaction energy is -53.5 and -43.5 kJ/mol for other cation pairs. The dispersion energy Edis is dominant among the other interaction energy.

Acknowledgments

The authors are grateful to their colleagues in the Institute of Bioorganic Chemistry of the Academy of Sciences of the Republic of Uzbekistan for supporting the X-ray experiment.

References

[1]. Robert H. Howland, MD.Methylene Blue: The Long and Winding Road from Stain to Brain: Part 1. J. Psychosoc. Nurs. Ment. Health Serv. 2016. 54(9), 21.

[2]. Kayabaşi Y., Erbaş O. (2020). Methylene blue and its importance in medicine. D. J. Med. Sci., 6(3), 136.

[3]. Oz M., Lorke D.E., Petroianu G.A. (2009). Methylene blue and Alzheimer's disease. Biochem Pharmacol. 78, 927.

[4]. Cannosa S., Bacchi A., Graiff C., Pelagatti P., Predieri G., Ienco A., Manca G., Mealli C. (2017). Hierarchy of Supramolecular Arrangements and Building Blocks: Inverted Paradigm of Crystal Engineering in the Unprecedented Metal Coordination of Methylene Blue. Inorg. Chem. 56, 3512.

[5]. Raj M.M., Dharmaraja A., Kavitha S.J., Panchanatheswaran K., Lynch D.E.(2007). Mercury(II)–methylene blue interactions: Complexation and metallate formation. Inorg.Chim. Acta. 360, 1799.

[6]. Sabirov V. Kh., Kadirova M. X. Z. (2022). Crystal structure of three chloridocuprate(I, II) complexes with methylene blue (MB) counterions. Naturforsch B. https://doi.org/10.1515/znb-2022-0146.

[7]. CrysAlis Pro Software System (version 1.171.40.84a), Intelligent Data Collection and Processing Software for Small Molecule and Protein Crystallography, Rigaku Oxford Diffraction: Yarnton, Oxfordshire (U. K.), 2020.

[8]. Dolomanov O. V., Bourhis L. J., Gildea R. J., Howard J. A. K., Puschmann H. (2009). OLEX2 A Complete Structure Solution, Refinement and Analysis Program. J. Appl. Crystallogr. 42, 339.

[9]. Sheldrick G. M. Acta Crystallogr. (2015). SHELXT-Integrated Space-Group and Crystal-Structure Determination. A71, 3.

[10]. Sheldrick, G. M. Crystallographic Computing. Ed. Moras D., Podjarny A. D., Thierry J. C. 1992, 145 - 157. IUCr. and OUP: Oxford, UK.

[11]. Spackman, P. R., Turner, M. J., McKinnon, J. J., Wolff, S. K., Grimwood, D. J., Jayatilaka, D., Spackman, M. A. (2021). CrystalExplorer: a program for Hirshfeld surface analysis, visualization and quantitative analysis of molecular crystals. J. Appl. Crystallogr. 54(3), 1006.

[12]. Spackman M. A., Jayatilaka D. (2009). Hirshfeld surface analysis. CrystEngComm. 11, 19.

[13]. Turner M J., Mckinnon J. J., Wolff S. K., Grimwood D. J., Spackman P. R., Jayatilaka D., Spackman M. A., CrystalExplorer 17.5. The University of Western Australia (2017).

[14]. McDowell J. J. H. (1976). The molecular and crystal structure of phenathiazine. Acta Cryst. 1976, B32, 5.

[15]. Rabinowich E.; Epstein L. Polymerization of Dyestuffs in Solution. Thionine and Methylene Blue. J.A.C.S. 1941. 63, 69–78.doi: 10.1021/ja01846a011

[16]. Florence Ng.; Naorem H. Dimerization of methylene blue in aqueous and mixed aqueous organic solvent: A spectroscopic study. J. Mol. Liq. 2014. 198, 255–258. doi: 10.1016/j.molliq.2014.06.030

[17]. Canossa S., Grai C., Crocco D., Predieri G. (2020). Water Structures and Packing Efficiency in Methylene Blue Cyanometallate Salts. Crystals, 10, 558; doi:10.3390/cryst10070558.

[18]. Kahn-Harari A., Ballard R. E., Norris E.K. (1973). The Crystal Structure of Methylene Blue Thioeyanate. Acta Cryst. B29, 1124.